Silicon (2013) 5:115–133
DOI 10.1007/s12633-012-9138-7

ORIGINAL PAPER

Transport of Dissolved Si from Soil to River: A Conceptual Mechanistic Model

Benedicta Ronchi · Wim Clymans · Ana Lúcia Pena Barão · Floor Vandevenne · Eric Struyf · Okke Batelaan · Alain Dassargues · Gerard Govers

Received: 12 March 2012 / Accepted: 3 December 2012 / Published online: 12 January 2013

Abstract This paper reviews the processes which determine the concentrations of dissolved silicon (DSi) in soil water and proposes a conceptual mechanistic model for understanding the transport of Si through soils to rivers. The net DSi present in natural waters originates from the dissolution of mineral and amorphous Si sources in the soil, as well as precipitation processes. Important controlling factors are soil composition (mineralogy and saturated porosity) and soil water chemistry (pH, concentrations of organic acids, CO_2 and electrolytes). Together with production, polymerization and adsorption equations they constitute a mechanistic framework determining DSi concentrations. We discuss how key controls differ across soil horizons and how this can influence the DSi transport. A typical podzol soil profile in a temperate climate is used as an example, but the proposed model is transferrable to other soil types. Additionally, the impact of external forcing factors such as seasonal climatic variations and land use is evaluated. This blueprint for an integrated model is a first step to mechanistic modelling of Si transport processes in soils. Future implementation with numerical methods should validate the model with field measurements.

Keywords Dissolved silicon · Si transport · Mechanistic Si model · Land use · Amorphous Si

B. Ronchi (✉) · W. Clymans · O. Batelaan · A. Dassargues · G. Govers
Earth and Environmental Sciences, K. U. Leuven, Celestijnenlaan 200E 2410, 3001 Heverlee, Belgium
e-mail: benedicta.ronchi@ees.kuleuven.be

A. L. P. Barão · F. Vandevenne · E. Struyf
Ecosystem Management Research Group, Department Biology, University Antwerp, Campus Drie Eiken, D.C.116, Universiteitsplein 1, 2610 Wilrijk, Belgium

O. Batelaan
School of the Environment, Flinders University, GPO Box 2100, Adelaide, SA 5001, Australia

A. Dassargues
Hydrogeology and Environmental Geology, Department of Architecture, Geology, Environment and Civil Engineering (ArGEnCo) and Aquapole, Université de Liège, B.52/3 Sart-Tilman, 4000 Liège, Belgium

1 Introduction

In aquatic systems, dissolved Si (DSi) is an important nutrient. Dissolved Si is mainly delivered to the oceans by river discharge. Rivers provide yearly 7.3 Tmol Si to estuaries from which ca 85 % consists of DSi. Eighty percent eventually reaches the ocean after passage through the coastal and estuarine filter, which corresponds to over 60 % of the total Si input into the oceans [1]. The remaining part is provided by eolian dust input and ocean floor weathering. The delivery of riverine Si to the oceans is critical for maintaining primary productivity in the world oceans and plays a crucial role in the biological uptake of CO_2 through the so-called biological carbon pump [2].

Land-river Si fluxes depend on the relative contribution of different Si sources and on the type of processes (e.g. biological, physico-chemical, pedological) occurring along the pathway [3, 4]. The particulate Si fraction in soils and bedrock consists of well-crystallized minerals (e.g. quartz, other primary and secondary silicates) and amorphous Si (ASi) [4, 5]. ASi can be subdivided in biogenic silica (mainly plant Si bodies called phytoliths)

and non-crystalline inorganic Si fractions (i.e. formed by pedogenic processes). Soils contain considerable amounts of biogenic Si (8250 Tmol Si) [6]. ASi is an important factor in Si release from soils for two reasons. Firstly, it is up to 17 times more soluble than quartz under laboratory conditions [7] and its dissolution may therefore constitute the most important source of DSi delivered to rivers by groundwater and/or surface and subsurface runoff [8]. Secondly, ASi may be directly delivered to aquatic systems by physical erosion during run-off events [9, 10].

DSi concentrations in soil water will have an important effect on the concentrations in and delivery to rivers of DSi. This is shown in runoff events, where river water often consists for a large part of water that is pushed out of the soil by the new precipitation event [11, 12]. Moreover, during base-flow river water consists mainly of groundwater that has previously percolated through soils. Understanding the mechanisms controlling DSi dynamics within soils is therefore key to understanding spatial and temporal variations of DSi in river water.

A wide range of processes other than mineral or ASi dissolution control soil pore water DSi concentrations: adsorption on Fe-and Al-oxides, polymerization, formation of nanocolloids, precipitation of secondary minerals and uptake by vegetation [4, 13–17]. At the landscape scale, geomorphological and hydrogeological features contribute to ASi and DSi reservoirs and hence to Si delivery. Land use can thus also strongly affect DSi delivery, as land use changes will not only affect vegetation but also soil hydrology [18] and soil chemistry [19–21]. Different processes have up to today been described separately by physically based equations but models integrating the various processes do not yet exist.

Si pools and fluxes in landscapes have previously been discussed in a review of Sommer et al. [3]. Street-Perrott and Barker [22] emphasized the importance of coupling the Si and C cycles, while Cornelis et al. [4] focused their review on the impact of the soil-plant system on DSi in weathering-limited and weathering-unlimited environments. While these reviews provide a good overview of the state of the art of our knowledge with respect to Si cycling, they do not discuss how this knowledge can be integrated in a mechanistic modeling framework that can be used to quantitatively predict (changes in) DSi concentrations and fluxes in soils as well as DSi delivery from soils to rivers. Other catchment studies developed empirical equations to calculate the DSi concentrations in groundwater and soil pore water based on measurements [8, 23]. However, these constitute site specific and non-transferable equations.

In contrast to earlier work, we here establish a framework of mechanistic equations that can be used to model DSi transport. An overview is given of all processes and equations describing ASi and mineral dissolution, DSi adsorption and uptake of DSi by plants. We also discuss further steps that are needed to develop a fully operational model of DSi production and delivery under different land uses. Finally, we discuss the relative importance of the different processes influencing DSi concentration and transport in each soil horizon of a typical podzol profile. The podzol profile is taken as an example to illustrate different processes. This blueprint of an integrated model is transferrable to different types of soils.

2 Sources and Sinks of Si in Soils

2.1 Typology of Si-particles

Silica is the second most abundant element in the earth crust and is present in different forms. In soils, mineral Si is dominant but amorphous Si (ASi) is also present in significant amounts [22]. A classification of all types of Si-particles is presented in Fig. 1. Mineral silicates can be subdivided in two categories, the primary minerals formed by magmatic crystallization (quartz, feldspars, ...) and the secondary minerals developed during soil formation. The secondary phases, concentrated in the clay fraction of soils, can be well crystallized like phyllosilicates [24], micro-crystalline (autigenic quartz, Opal CT, chalcedon) or short-range ordered (imogolite, proto-imogolite, allophane) [25–27]. Amorphous forms of non-biogenic Si are non-crystalline inorganic particles forming opal-A or volcanic glasses. Amorphous coatings of opal can also cover secondary minerals [15, 28]. Amorphous Si can also be of biogenic origin. In this biogenic Si pool, the phytogenic Si (including phytoliths) is the most important component. Phytoliths are formed by plants taking up DSi from the soil solution, which then precipitates as phytoliths in plant roots, stems and leaves/needles. When dead plant material is decomposed, the phytoliths are deposited in the topsoil. Phytoliths are not the only important form of biogenic ASi in soils, also sponge spicules, diatoms and testate amoebae are important components of biogenic Si [3, 5], especially in wetlands [29] and forests [30]. As the crystallinity varies for the different types of Si-particules, their relative stability against weathering

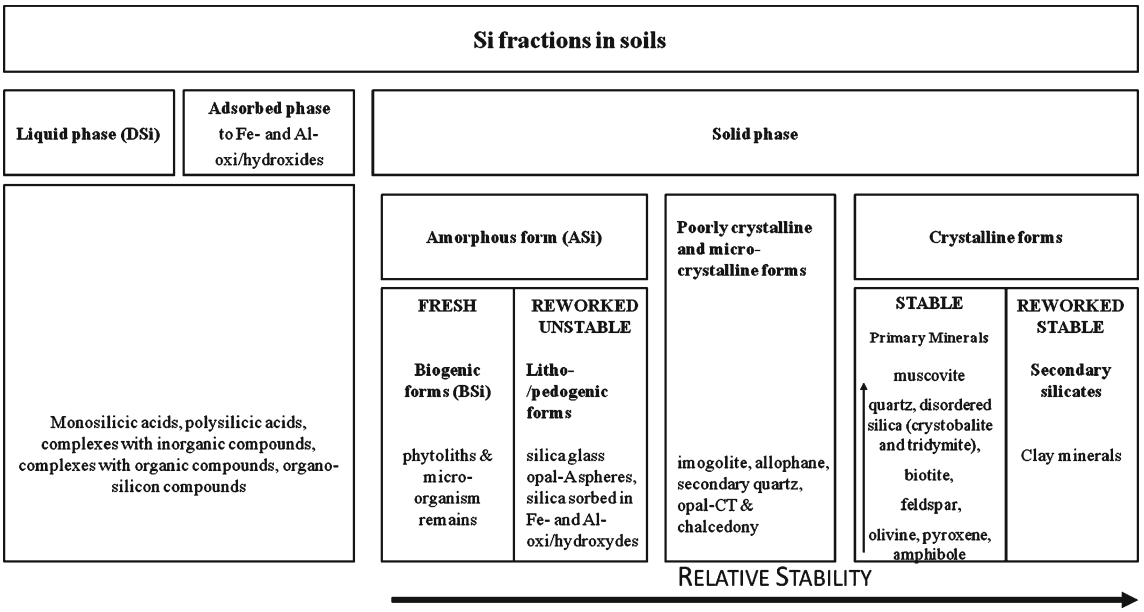

Fig. 1 Classification of Si compounds present in soils. Arrows show increasing stability of solid compounds against weathering [4, 5]

also differs (Fig. 1). An extensive review of all different types of Si is given in Cornelis et al. [4] and Sommer et al. [3].

2.2 Si Dissolution and Weathering

Si concentration in natural waters is often considered to be mainly controlled by mineral silicate hydrolysis (Eq. 1), i.e. 45 % of the total dissolved load (for all elements) in rivers is attributed to mineral silicate weathering [31]. The dissolution of silicates and amorphous Si forms monosilicic acid (H_4SiO_4; DSi)

$$SiO_{2(s)} + 2H_2O_{(aq)} \leftrightarrows H_4SiO^0_{4(aq)} \tag{1}$$

Dissolution can also lead to the formation of polysilicic acid, but its stability is relatively low [32].

In contrast to quartz, which is highly ordered, amorphous silica is a short-range order crystal composed of loosely packed silica tetrahedrals. Consequently, the solubility of amorphous silica is higher (1.8–2.1 mM Si for synthetic ASi and 0.02–0.36 for BSi) than that of quartz (0.03–0.25 mM Si). Since surface coatings often cover quartz grains in soils, low mineral solubility values generally apply to soils [3].

The mass-balance for a specific element in an aqueous solution resulting from dissolution of mineral phases can be calculated for i reactants and p product phases as

$$\sum_{j=1}^{i} MTC_p \alpha_p^i = \Delta m_i = m_{i(final)} - m_{i(initial)} \tag{2}$$

Where MTC is the mass-transfer coefficient for any phase (p) in moles, α the stoichiometric coefficient of element i in phase p and m the total moles of element i in the initial and final solutions [33, 34].

Si solubility is relatively constant between pH 2 and 8.5 but increases drastically when pH > 9 or pH < 2 [34, 35]. Alkaline conditions increase dissolution of ASi, imogolite and allophane while acidic conditions increase the desorption of adsorbed Si [5]. Gérard et al. [8] take account of pH, reactive surface and the temperature dependency of the Arrhenius equation (Eq. 4) when calculating the Si dissolution rate constant for silicate minerals as

$$r_d = k_d S \left\{H^+\right\}^n \left(1 - e^{-A_r/RT}\right) \tag{3}$$

with

$$A_r = -RT \ln\left(\frac{Q}{K}\right) \tag{4}$$

in which r_d is the dissolution rate (mol kg^{-1} s^{-1}), k_d is the dissolution rate constant (mol m^{-2} s^{-1}), S is the reactive surface of the mineral (m^2 (kg $H_2O)^{-1}$), {H+} is the activity of protons in the reacting solution, n is an experimental exponent, Q is the ionic activity product and K the equilibrium constant of the reaction. The temperature dependence of k_d is described by

$$k_d\,(T) = k_d^0 e^{-E_a/RT} \tag{5}$$

Here k_d^0 is k_d at a given reference temperature, E_a is the apparent activation energy of the dissolution reaction

(kJ mol^{-1}), R is the gas constant (8.32 × 10^{-3} kJ mol^{-1} K^{-1}) and T is the temperature (K).

The equations above describe the mineral dissolution in deionized water. However, the presence of electrolytes can increase dissolution rates. Water dipoles can more easily attack mineral surfaces on which cations are adsorbed [36]. To correct for this, the Langmuir adsorption model can be integrated [37] in Eq. 3

$$k_d^{corr} = k_d^{Na^+}\sigma_{Na^+} + k_d^{Mg^{2+}}\sigma_{Mg^{2+}} + k_d^{Ca^{2+}}\sigma_{Ca^{2+}} + k_d^0\left[1 - \left(\sigma_{Na^+} + \sigma_{Mg^{2+}} + \sigma_{Ca^{2+}}\right)\right] \quad (6)$$

with

$$\sigma_A = \frac{K_{ad}^A m_A}{1 + K_{ad}^{Na^+} m_{Na^+} + K_{ad}^{Mg^{2+}} m_{Mg^{2+}} + K_{ad}^{Ca^{2+}} m_{Ca^{2+}}} \quad (7)$$

Where σ_A is the fraction of sites occupied by cation A, m_A the molal concentration of the cation and K_{ad}^A the equilibrium adsorption coefficient of the cation. The last term of Eq. 6 allows accounting for adsorbed H^+ protons, which were not replaced by cations as their adsorption is a competitive process [38].

In natural waters, not only electrolytes are present but also CO_2 is dissolved in the water and influences Si weathering processes

$$CaAl_2Si_2O_8 + 2CO_2 + 8H_2O \leftrightarrows Ca^{2+} + 2Al(OH)_3 + 2H_4SiO_4^0 + 2HCO_3$$

Consequently, water acidification by CO_2 production $\left(P_{CO_2}^m\right)$ as well as the presence of organic acids (*org*) need to be accounted for [39, 40]

$$r_j = k_{H^+}\frac{\{H^+\}^n}{\{M\}^x\{Al^{3+}\}^y} + \frac{k_{H_2O}}{\{Al^{3+}\}^u} + k_{CO_2}.P_{CO_2}^m + k_{org}\left[org\right]^{0.5} \quad (8)$$

Where r_j is the dissolution rate of mineral j, k_i is the rate coefficient, *M* the base cations (Ca^{2+}, Mg^{2+}, Na^+ and K^+), and *n, x, y, u* and *m* apparent reaction orders to be determined experimentally. Similar as in Eq. 3, the first term of the Eq. 8 accounts for the effect of pH and solution composition, while additionally the effect of Al^{3+} is introduced. This term stands for formation and decomposition of activated surface complexes. The concentrations of base cations and Al are pH-dependent, in acid water the base cations on the exchange complex are replaced by H_3O^+ [41, 42] and $Al(OH)_3$ dissolution is enhanced. After the replacement of exchange complexes by H_3O^+, an alkali-depleted layer enriched in Si and/or Al forms around the mineral. This residual layer will dissolve slowly. Al therefore has a complex role in the dissolution of minerals as its concentration is not only pH-dependent (like showed in the first term) but also interacts in the residual layer [43], the third term of Eq. 8 accounts for this interaction. The last two terms calculate the rate contribution of acidification factors [33].The presence of CO_2 accelerates the dissolution by providing protons [44]. Berg and Banwart [45] suggest that at neutral to near basic pH, weathering is enhanced by the reactive carbonate complexes adsorbed on mineral surfaces. The presence of organic acids can also significantly increase dissolution rates by lowering the pH but this process seems only to be significant below pH 5 [46]. Organic acid influence on silicate weathering is indirect, secondary iron and aluminium hydroxides dissolve first. In aluminosilicates the Al-O bounds will break more easily than the stronger Si-O bounds [47–53]. The resulting higher permeability induces an accelerated transport through the soil thereby increasing also weathering.

In the equations above, water availability is assumed non-limiting. However, dissolution and hydrolysis require contact between water and minerals. It can thus be assumed that the total weathered amount (R_w) within a soil profile is proportional to the soil water content (θ) as well as the time (t) of the weathering processes [33]. As the soil composition and water content vary from one horizon to another, the total weathering rate has to be calculated for each horizon and finally summed for the whole soil column.

$$R_w = \sum_{i=1}^{horizons}\theta_i \sum_{j=1}^{\min erals} r_j.t \quad (9)$$

Weathering processes of silicates are generally accelerated in the vadose zone, especially in the root zone where biological activity is important [54, 55]. This is mainly related to higher productions of CO_2 and organic acids (Eq. 8) by roots in the unsaturated zone, which effect is summed up for each mineral (Eq. 9). Silicate weathering also increases with increasing concentrations of H_2CO_3 and H_2SO_4 [56, 57]. These acids are produced in the saturated zone by mineralization processes of organic compounds and sulfide oxidation respectively [57]. The effect of H_2CO_3 is the same process as observed by Berg and Banwart [45] and is accounted for in Eq. 8 by the third term. However, the effect of H_2SO_4 on Si weathering has hitherto never been formulated in a similar equation.

The combination of existing knowledge, as presented above, allows us to propose a new set of equations to approximate the amount of Si dissolved in soil from a diverse range of sources.

$$r_{d\ total} = \sum_{j=1}^{horizons}\left(\theta_j \sum_{i=1}^{soil\ comp}\alpha_i r_{d_i}\right) \quad (10)$$

$$r_{d\,hor} = \theta \sum_{i=1}^{soil\ comp} \alpha_i r_{d_i} \tag{11}$$

$$r_{d_i} = k_d^{corr}\, S \left\{H^+\right\}^n \left(1 - e^{-A_r/RT}\right) \times \left(\frac{k_{H_2O}}{\left\{Al^{3+}\right\}^u} + k_{CO_2}.P_{CO_2}^m + k_{org}\left[org\right]^{0.5} + \mathrm{k}_{\mathrm{SO}_4^{2-}}\left[\mathrm{SO}_4^{2-}\right]^{\mathrm{a}} \right) \tag{12}$$

With

$$k_d^{corr} = \left(\sum \sigma_{\mathrm{A}} \mathrm{k}_{\mathrm{d}}^{\mathrm{A}}\right) + k_d^0 \left[1 - \left(\sum \sigma_{\mathrm{A}}\right)\right] \tag{13}$$

Where A = Na^+, Ca^{2+}, Mg^{2+}, K^+ and Al^{3+}.

Knowing the *fraction* of each soil component in the soil (α in %), a weighted rate $r_{d\,hor}$ can be calculated for each soil horizon j. As k_d^0 is different for each source type, r_d has to be calculated for each Si soil component $i\,(r_{d_i})$, in other words for each mineral. The $r_{d\,total}$ is then the rate for the whole soil profile.

Current approaches modeling DSi dynamics generally ignore the ASi pools as potential DSi sources and/or DSi sinks. This strongly contrasts with available field evidence, ASi was found to be the principal DSi source in leaching water and stream water in different areas [58, 59]. While there is ample evidence showing that the plant reservoir is important, very little quantitative information is at present available with respect to the relative contribution of biogenic and mineral Si to DSi in soil water for natural and cultural ecosystems. The few studies that have been realized on the reactivity of ASi show complex dissolution rates. Saccone et al. [60] tested different Si extraction techniques and concluded that phytoliths dissolve more easily in alkaline solutions while adsorbed and mineral Si were extractable with acid solutions. The substitution of Si by Al at the surface of BSi particles lowers it reactivity [61]. Loucaides et al. [62] showed a positive correlation between dissolution rates and deprotonated silanol (SiO^-) groups, which are present at the outer surface of phytoliths at pH higher than 2.5–3. Given the importance of these processes and the variable composition of the biogenic ASi soil pool (phytoliths of different plant species, testae, spicules, ...), it can be assumed that there is a large range of biogenic ASi reactivities [63]. We assume we can use Eq. 12 for biogenic ASi when using an appropriate k_d-value. Although, future research should investigate if ASi dissolution is influenced by the adsorption of base cations and Al^{3+} (Eq. 13) and by similar state variables as those included in the last factor of Eq. 12 (Al^{3+}, pCO_2, [org], SO_4^-). This should confirm whether Eq. 10 can be extended to include ASi dissolution and reprecipitation as pedogenic ASi, which can then again be subjected to dissolution.

2.3 Sinks of DSi

Si is not only released in water of natural systems but it can also: (1) be adsorbed to soil components; (2) form nanocolloids by polymerization; (3) take part in neoformation and precipitation as secondary minerals; and (4) actively be precipitated in vegetation as phytoliths.

(1) Monosilicic acid (H_4SiO_4) sorbs on solid phases, mainly on Fe- and Al-oxides and hydroxides. The amount of adsorbed Si increases when pH increases from 4 to 9 [15, 32, 64] and can be quantified with a charge distribution model [65]. Thermodynamically the adsorption can be calculated as:

$$\left(\frac{\delta \log \mathrm{C}_{Si-tot}}{\delta pH}\right)_{\Gamma_{Si}} = \left(\frac{\delta \Gamma_H}{\delta \Gamma_{Si}} - n_H\right)_{pH} \equiv (\chi_H - n_H)_{pH} \tag{14}$$

in which $\left(\frac{\delta \log \mathrm{C}_{Si-tot}}{\delta pH}\right)_{\Gamma_{Si}}$ is the ratio between the change of the total concentration of DSi (C_{Si-tot}) and the change of pH at a constant silicate loading, Γ_{Si}; $\frac{\delta \Gamma_H}{\delta \Gamma_{Si}}$ is the ratio of change of the proton adsorption over the change of the silicate adsorption; n_H is the proton balance in the solution and χ_H is the proton co-adsorption ratio. Equation 14 implies that the concentration change is equal to the change in H+ adsorption (Γ_H) as result of the adsorption of Si at the surface (Γ_{Si}) at a given constant pH after correction for the mean relative number (n_H) of protons present on the species in solution at that pH. The n_H and Γ_H are calculated for the chosen reference species of DSi, $H_4SiO_4^0$. This is the most common species at pH below 9, which means $n_H = 0$ when the pH < 9. If $H_3SiO_4^{-1}$ is the only Si species present in significant concentration at pH > 9 values, n_H will be equal to −1 [66, 67].

(2) It is generally admitted that polysilicic acid decomposes easily in monomers but depending on the environmental conditions, depolymerisation of polysilicic acid takes place in a few hours, days or months [32]. Monosilicic acid ($H_4SiO_{4(mono)}$) forms critical nuclei that rapidly develop into nanocolloids ($H_4SiO_{4(nano)}$) by oligomerization. In natural environments, up to 65 % of total aqueous silica can be composed of nanocolloidal silica [16]. If the nanocolloids aggregate, SiO_2

precipitates [68–71] and forms ASi particles. Polymerisation of these oligomers takes place in acidic and neutral environments (2 < pH < 7) [68–71]. High amounts of nanocolloidal silica are present in environments with low pH (3–4) and at neutral pH in combination with a low ionic strength. In acidic environments the concentration of monomeric Si is in equilibrium with the concentration of nanocolloidal Si. The conversion of nanocolloidal Si to precipitated Si is limited in these conditions in contrast to environments with neutral pH [16]. In basic conditions (pH < 9), monosilicic acids are negatively charged. Electrostatic forces then prevent polymerization except when the presence of metal cations allows neutralizing the monomers [68–71]. To simulate the concentrations of monomeric ($[SiO_{2(mono)}]$) and nanocolloidal SiO_2 ($[SiO_{2(nano)}]$) (a supersaturation model (Eqs. 15 and 16) was proposed by Conrad et al. [16].

$$[SiO_{2(mono)}] = \left(3k_1 t + \frac{1}{([SiO_{2(mono)}]_{t=0} - [SiO_{2(eq)}])^3}\right)^{-1/3} + [SiO_{2(eq)}] \quad (15)$$

and

$$\frac{d[SiO_{2(nano)}]}{dt} = \frac{1}{4}k_1\left[\left(3k_1 t + \frac{1}{([SiO_{2(mono)}]_{t=0} - [SiO_{2(eq)}])^3}\right)^{-1/3} + [SiO_{2(eq)}]\right]^4 - k_2[SiO_{2(nano)}]^m \quad (16)$$

With $[SiO_{2(eq)}]$ the equilibrium concentration of precipitated amorphous SiO_2, k_1 the reaction rate constant for the formation of critical nuclei, k_2 the rate of precipitation and m the reaction order with respect to $SiO_{2(nano)}$.

(3) Processes of pedogenic formation of secondary minerals (phyllosilicates, silica and short-range ordered aluminosilicates) depend on DSi concentrations in the soil pore water. High Al disponibility favorises clay formation [72], under such conditions, short-range ordered Al-Si compounds (hydroxyaluminosilicates, HAS) are formed in soils with pH > 5 [26]. HAS are amorphous precursors of imogolite [13, 73]. In presence of active organic matter, the formation of allophane and imogolite is suppressed as Al preferentially forms complexes with organic matter in those conditions. As a consequence, opaline silica precipitates [74]. In soil conditions, HAS form preferentially when soil moisture conditions are dry, organic matter mineralises and the roots and micro-organisms are active [75]. This is an example of the fact that for the precipitation of each secondary mineral, specific equilibrium conditions need to be reached.

(4) The DSi uptake by plants can be higher (active uptake) than, proportional to (passive uptake) or lower than (active exclusion), the predicted uptake by water mass transfer. Lower uptake leads to H_4SiO_4 accumulation in the soil. Cornelis et al. [4] reviewed the literature on Si accumulation in plants and showed that both the main source and sink for DSi in soil solutions are phytoliths. Farmer et al. [58] showed that the dissolution of phytoliths stored in soil were the main contributor to DSi in the river water during winter rains and spring snowmelt [58].

To calculate the active uptake of Si the Michaelis-Menten (Monod) rate (Eq. 17) can be used.

$$r_a = k_M\left(\frac{[Si]}{K_M + [Si]}\right) \quad (17)$$

where r_a is the active uptake of DSi (mol L^{-1} s^{-1}), k_M is the kinetic constant (mol L^{-1} s^{-1}) and K_M is the half saturation constant (mol L^{-1}). This equation is commonly simplified to a first order rate equation (Eq. 18) by attributing a high value to K_M.

$$r_a = \frac{k_M}{K_M}[Si] \quad (18)$$

Active uptake will lower the Si concentration in soil pore water and the DSi concentration in receiving rivers may therefore be expected to decrease during periods of active DSi uptake by terrestrial vegetation [76]. On the contrary, the DSi concentration will not vary seasonally in the case of passive uptake provided that the flux of passive uptake is the product of the DSi concentration and the transpiration flux.

2.4 Towards an Integrated Conceptual Model

Only one attempt has been made to simulate the net effect of both sinks and sources on the final DSi concentration in the soil solution in a forested environment, and we have no knowledge of such efforts in

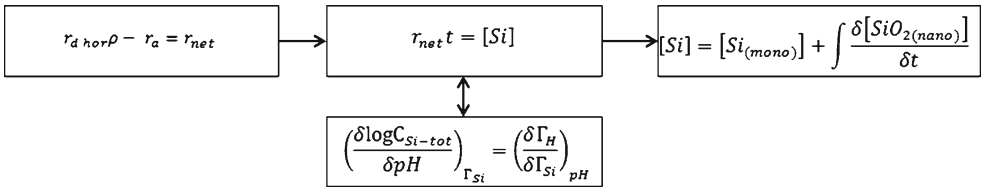

Fig. 2 Blueprint of the estimation procedure for Si concentration in soil water and groundwater by taking into account dissolution and sink processes. This conceptual model is based on Eqs. 10, 14, 16 and 17

other vegetation types. Gérard et al. [77] proposed a conceptual model and simulated it using the MIN3P code [78], in which active and passive uptake of Si were integrated. In this specific case study, soils did not contain evidence of secondary mineral precipitations. Consequently, the model was build based on the hypothesis that uptake was the only possible sink process. However, evidence for other sink processes (e.g. nanocolloid formation) was not investigated. We propose a conceptual model for future Si concentration calculation models by coupling all known equations expressing Si dissolution and sink processes (Fig. 2). In contrast to existing models, this conceptual model includes all known sink processes. The development of such a model should allow to estimate the importance of specific dissolution and sink processes, even in fields where soil solution and soil analysis show no clear evidence of the controlling process (e.g. for soils containing ASi, Al- and Fe-oxides and HAS with soil solutions showing no clear seasonal variation and/or containing nanocolloids).

The blueprint of our model is presented in Fig. 2. Firstly, mineral dissolution in a specific soil horizon is calculated by obtaining r_d from Eq. 11, which is subsequently multiplied by the bulk density (ρ) of the soil horizon. In the case of active uptake, the uptake by vegetation (described by r_a) has to be accounted for in the root zone using Eq. 17. The obtained value (r_{net} in mol L^{-1} s^{-1}) is then multiplied by the duration of a time step (t in s) to obtain the gross increase in DSi concentration, after which losses due to the adsorption of Si are estimated using Eq. 14. The final Si concentration obtained is the total of monomeric and nanocolloidal SiO_2. Estimating the relative importance of both fractions with Eqs. 15 and 16 requires to calibrate the result by measuring the monomeric SiO_2, e.g. with the molybdenum blue method [24]. This Si model needs to be coupled with a water flux model, not only to estimate active uptake, but also to simulate Si fluxes between different soil horizons.

To illustrate the relative importance of all the processes in different types of horizons, we describe our conceptual model for a podzol soil system, assuming passive Si uptake by vegetation ($r_a = 0$) (Fig. 3) and steady-state downward water flow (Figs. 3 and 4). As water is flowing downward through the soil profile, the DSi concentration in a particular horizon results from the sum of the DSi concentration measured in the horizon above and the produced or deposited DSi in the considered horizon. Assuming dissolution processes are generally more important than sink processes, the simulated DSi concentration builds up with depth (Fig. 3). The relative importance of the parameters (Table 1) from our model (Fig. 2) depends on the active processes in a specific horizon. Simultaneous mobilization of Si in the humus layer is expected from the following processes: dissolution, transfer with upward capillary movement and uptake

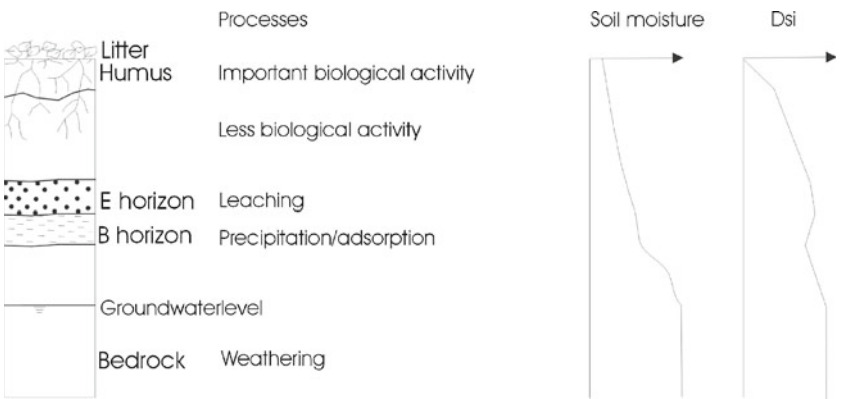

Fig. 3 Typical podzol soil profile in temperate climate. Processes and soil moisture vary with depth from one horizon to another. The relative importance of DSi is plotted for this soil covered by vegetation with a passive uptake of Si and with important adsorption and precipitation processes in the B horizon

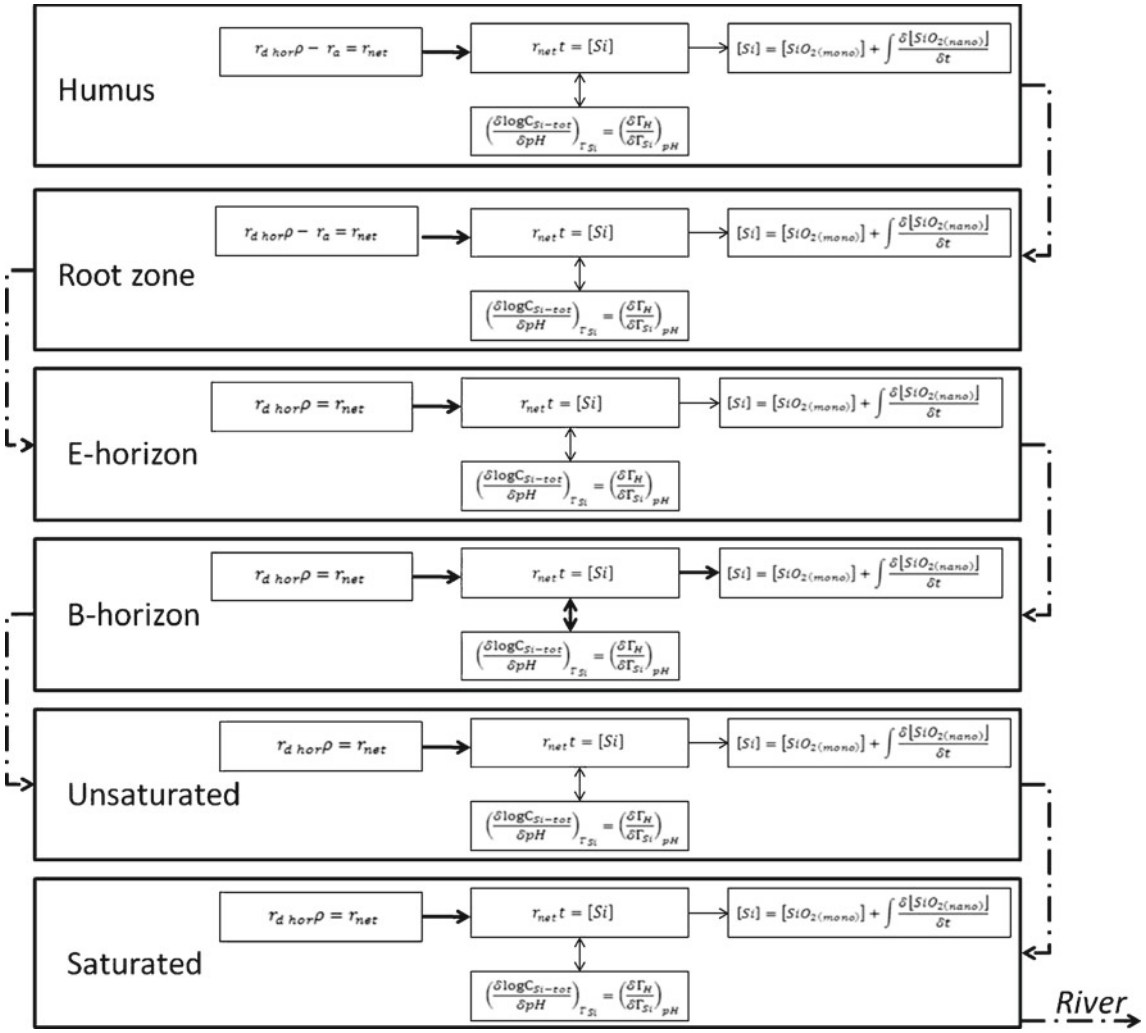

Fig. 4 Conceptual model of the transport of DSi through each horizon of a podzol soil. Each box is a horizon with dissolution and sink processes of different relative importance (thick arrow: important process). Dashed arrows show the transport from one horizon to another with the river as final receptor

by roots and mycorrhizal hyphae. Site specific conditions will determine the relative importance of these mechanisms [59]. The concentration of organic acids, BSi and pCO_2 (Eq. 12) are important in the humus layer and in the root zone (A horizon), which should lead to a rapid Si dissolution (Fig. 3). For the humus layer of podzolic soils, low molecular weight organic acids (LMWOA) concentrations range between 501

Table 1 Relative importance of parameters of Eqs. 10, 12 and 17 for each soil horizon for a soil profile like presented in Fig. 3

		r_d				θ	r_a^1
		$[H+]^1$	pCO_2^1	$[org]^1$	$[SO_4^{2-}]$		
Unsaturated	Humus	+++	+++	+++	0	$< \Phi$	±
	A horizon	++	++	++	0	$< \Phi$	±
	E-horizon	+	+	±	0	$< \Phi$	0
	B-horizon	−	±	±	0	$< \Phi$	0
Saturated zone		±	$\pm/+^2$	±	±	Φ	0

+++, ++, +, ±, − is the scale from very important to unimportant. 0 stands for negligible and ϕ for porosity

[1]This factor needs to be taken into account if uptake is active and only in the root zone.[2] pCO_2 increase in the saturated zone in case of carbonate bedrocks, which produce bicarbonate acids by weathering

and 2644 μM, pH varies between 3.0 and 3.8, while DSi ranges between 25–353 μM [79].

In the E-horizon most soluble particles have been leached out and only the most stable minerals are left. Based on our conceptual model, we assume this should lead to a limited increase or to no further change in DSi concentration in this horizon (Fig. 3). For podzolic soils, LMWOA concentrations ranged from 0.00 to 450 μM, pH from 2.6 to 4.0 and DSi from 103 to 1032 μM in the E-horizon. In the B-horizons of these soils, LMWOA concentrations ranged from 0 to 124 μM and pH from 4.4 to 6.7 [79]. As the acidity is lower in the B-horizon than in the overlying horizons, parameters $\{H^+\}$ and $[org]$ (Eq. 12) diminish resulting in a lower dissolution rate r_{d_i} (in Eq. 12). Resulting DSi concentrations in soil water are generally lower in the B-horizon (116–351 μM in [79]) than in the E-horizon. In the B-horizon DSi can be adsorbed due to the higher concentration of Al- and Fe-hydroxides (Eq. 16) and oxides and precipitation of secondary minerals can take place (Figs. 3 and 4). The concentrations of Al and base cations (Eq. 12) are therefore likely most important in the B horizon. To complicate the situation the presence of organic acids, pCO_2 and ASi needs to be accounted for when root zones extent into the E- and B-layers. In that case concentrations of organic acids and ASi will be higher over a deeper section of the soil profile. Finally, DSi concentrations depend on the importance of each of the processes described. In the upper part of the soil profile the poorly known biological and pedogenic processes probably control the Si-cycle, in topsoils ASi particles are biogenic while pedogenic Si is likely more important deeper in the profile, even in presence of roots [80].

Deeper in the soil, geological processes as e.g. weathering of minerals are controlling Si-transport, these processes have been studied in detail. We assumed in our conceptual model (Fig. 3) homogeneous bedrock, it is also realised that we should account for sulfates and carbonates (pCO_2) in the saturated area when using Eq. 12.

Soil moisture will depend on soil texture, θ will typically range between 0.25–0.45 in silt and between 0.1–0.4 in sandy loam. Clay richer B-horizons have a bigger retention capacity providing higher θ values [81]. In the capillary fringe located just above the groundwater level, θ increases strongly (Fig. 3) and approximates saturation, i.e. ϕ (Table 1). This increased soil moisture will facilitate dissolution (Eqs. 9, 10 and 11) as well as DSi diffusion from capillary to leaching pore water. The relative water content profile represents an average situation, but in dry or wet conditions the top of the profile certainly differs.

For the podzol soil profile illustrated in Fig. 3, we propose a conceptual model as presented in Fig. 4 whereDSi concentrations are calculated for each soil horizon. Dissolution processes are dominant in the soil profile, except in the B-horizon where adsorption can play an important role (Fig. 4). As both soil moisture and DSi concentrations are increasing with depth, the adsorption and precipitation horizons are likely an essential filter on the eventual export of DSi from the soil profile to rivers.

Based on the blueprint of our model (Fig. 2), we can make similar models as Fig. 4 for other soil profiles. Generally at the top of podzols, a litter layer is present [82] which contains BSi. However, for soil profiles without a litter layer we expect lower amounts of BSi. Moreover since non-podzolic soils are less acidic [82], we can expect lower DSi concentrations. On the other hand given that there is no E-horizon, the DSi increase along the depth should be more constant than for podzols. The composition of the B-horizon (e.g. content of organic acids, of ASi, of Al- and Fe- oxides, mineralogy, etc.) will determine which dissolution/sink processes are important and thus control the DSi concentrations. In other words, in a box model like Fig. 4 for a non-podzolic soil, the box "E-horizon" should be suppressed and the thickness of the arrows in the box "B-horizon" adapted in function of the observed key controlling processes.

3 Delivery of Si from the Soil to the River

Biogeochemical mass balances of Si have been established on the ecosystem scale [83, 84]. As these models are based on steady state assumptions processes leading to DSi export are *hitherto* excluded. However, steady state assumptions for soils and vegetation are difficult to maintain, especially for small-catchment studies [83]. In these head-waters, it is necessary to focus on the dynamics of the processes in the unsaturated and saturated zone. Within these zones the effective transport of DSi will depend on soil hydraulic parameters like the hydraulic conductivity, which depends on θ in the unsaturated zone, porosity, bulk density, matrix tortuosity, dispersivities, effective diffusion coefficient and adsorption partitioning coefficient of the different soil horizons [85].

Graf and Therrien [37] simulated the transport of DSi with thermohaline groundwater flow at the catchment scale in 3D, focusing on groundwater flow and saturated ($\theta = 1$) conditions, neglecting plant uptake. They included the effect of adsorption by use of a retardation factor. Their reactive transport

model for DSi is expressed in Eq. 19, which assumes fluid incompressibility and constant fluid density [85].

$$\frac{\delta\left(R\phi C\right)}{\delta t} = \frac{\delta}{\delta x_i}\left(\phi D_{ij}\frac{\delta C}{\delta x_j} - q_i C\right) + \Gamma_m \tag{19}$$

In Eq. 19, i and j are the dimension and equal to 1, 2 or 3, q_i is the Darcy flux (m s^{-1}) which depends on the hydraulic conductivity of the soil, C (kg l^{-3}) is the solute concentration, R (−) is the retardation factor, D_{ij} (m^2 s^{-1}) is the coefficient of hydrodynamic dispersion, Γ_m (kg l^{-3} s^{-1}) is the source/sink term or the net production of H_4SiO_4.

$$\phi D_{ij} = \left(\alpha_l - \alpha_t\right)\frac{q_i q_j}{|q|} + \alpha_t |q| \delta_{ij} + \phi\tau D_d \delta_{ij} \tag{20}$$

$$R = 1 + \frac{\rho_b}{\phi} K_d \tag{21}$$

The coefficient of hydrodynamic dispersion D_{ij} is given by Bear's equation (Eq. 20) [85] where α_l (m) and α_t (m) are respectively the longitudinal and transverse dispersivity, τ is the matrix tortuosity, D_d (m^2 s^{-1}) is the free-solution diffusion coefficient and δ_{ij} (−) is the Kronecker delta function. The transport will also be retarded partly due to adsorption. The retardation factor R defined in Eq. 21 [86] depends on the bulk density ρ_b (g m^{-3}) of the porous medium and the equilibrium distribution coefficient K_d (g^{-1} m^3) for a linear Freundlich isotherm.

While Graf and Therrien [37] studied the transport of DSi only for the saturated zone, Gérard et al. [8] investigated processes controlling DSi on the scale of the soil profile, in the unsaturated zone. DSi concentrations were analysed in leachates and in capillary solutions. The seasonality in DSi differed between capillary solutions and leaching solutions, with maximum DSi values observed in different seasons. DSi concentrations in capillary solutions were mainly controlled by surface weathering, with slow diffusion to leaching solutions. Gérard et al. [8] suggest that diffusion goes more rapidly in well drained systems, like those studied by Berner et al. [87]. In Gérard et al. [77] the flux is simulated based on Eq. 22 through the first 120 cm of a topsoil covered by a forest.

$$\frac{\delta\left(\theta\phi C\right)}{\delta t} = \frac{\delta}{\delta x_i}\left(\theta\phi D_{ij}\frac{\delta C}{\delta x_j} - q_i m\right) + \Gamma_m - q_p C \tag{22}$$

with

$$D_{ij} = \left(\alpha_l - \alpha_t\right) q_i + D_d \tag{23}$$

In this zone and on this scale the uptake flux (q_p [s^{-1}]) of the solute (C [mol l^{-1} s^{-1}]) by vegetation will have an influence on the Si transport. However, when active uptake is observed, the model also includes Eq. 17. The soil moisture is taken into account, (Eq. 22) as the topsoil is located in the partially saturated zone and since transport can only take place if enough water is available. For the 1D simulation of Si flux through vertical soil profiles, the equation for the hydrodynamic dispersion coefficient D_{ij} (Eq. 20) has been simplified (Eq. 23). Retardation is not taken into account in this study [8].

To simulate all processes on a catchment scale, we propose to use Eq. 24 as a combination of Eqs. 19 and 22.

$$\frac{\delta\left(\theta R\phi C\right)}{\delta t} = \frac{\delta}{\delta x_i}\left(\theta\phi D_{ij}\frac{\delta C}{\delta x_j} - q_i m\right) + \Gamma_m - q_p C \tag{24}$$

In the partially saturated zone (upper part of Figs. 3 and 4), θ is lower than 1 as opposed to the saturated zone where it is equal to 1 (lower part of Figs. 3 and 4). Hence, q_p will be greater than 0 in the root zone (Figs. 3 and 4) in contrast to the zone below the roots where it is equal to 0. For the hydrodynamic dispersion coefficient D_{ij} it is recommended to use Eq. 20, at least if all parameters can be estimated. In the podzol profile represented in Fig. 3, water transports concentrations (Eq. 24) from one horizon to another as illustrated by the dashed arrows in Fig. 4. While the saturated zone is assumed to have a homogeneous lithology, the DSi concentrations calculated in the final box should be similar to the DSi concentrations in the river during base flow. Here the transport Eq. 24 is also used with θ equal to ϕ.

4 External Forces Altering Internal Dynamics

4.1 Effect of Land Use

Land use has an impact on different state variables in the soil-vegetation continuum (soil structure, vegetation, hydrology, etc.), and it is therefore clear it will impact Si dynamics.

Weathering rates and the internal biogeochemical cycle of Si depend directly on the type of vegetal cover (quality and quantity of roots). Vegetation alters physical soil properties: (1) reactive surface area; (2) soil temperature; and (3) susceptibility for erosion. The reactive surface area is controlled by vegetation through binding fine particles and disintegrating bedrock [20], in turn altering the interaction potential between soil ASi and mineral Si and water. Vegetation also impacts soil temperature variability [88] and chemical properties of the soil solution [21, 89]. Plants and associated micro-

biota generate chelating ligands and acidifying products like CO_2 and organic acids (Eq. 12). The effect of land use on final Si delivery to riverine systems is corroborated by various studies that showed that Si export fluxes from different ecosystems vary significantly [90–92]. To take into account the role of ecosystems as filters in the Si transport [63], we show for the three most common temperate land use types (croplands, forest and grasslands) how DSi concentrations and the state variables of Eq. 12 are influenced by land use (Fig. 5).

Before discussing the three typical land use types it is important to underline that the model was exemplary constructed to describe a podzol profile. Podzols with their characteristic eluviation (E) horizon are typically acidic soils (pH < 5), and are considered to be unsuitable for agricultural practices (needs a pH > 5), and therefore mainly covered by forests. Agricultural areas, like cropland and grassland, are rarely situated on podzols, but are preferentially on soil types like (albe-)luvisols, fluvisols, gleysols etc. with a typical (ABC-profile). The strength of our conceptual model, that incorporates the presence of an E horizon, is that it easily can be transformed to other soil types, which lack an E horizon. The separation of Si reactions per horizon, and exchange between horizons, based on specific chemical, physical and biological properties of each horizon (Fig. 4) makes it possible to eliminate or incorporate horizons in the model. In the case of land use conversion, we eliminated the E horizon as farmers have preferentially used non-acidic soil for agricultural activities (Fig. 5).

4.1.1 Forests

Forests are characterized by an important internal biogeochemical (re-)cycling of Si which reaches the deeper the soil horizons. In temperate forests, vegetation uptake (Eq. 17 if active) ranges from 2.3 to 43 kg ha^{-1} yr^{-1}, Si restitution by litterfall ranges from 2.1 to 41 kg ha^{-1} yr^{-1}, and the export by drainage (Eq. 24) from the catchments is ranging from 0.7 until 28 kg ha^{-1} yr^{-1} [77, 93–95]. Due to this intensive internal cycling, the transport of DSi towards the river is delayed [96]. Further the Si concentrations within the profile are largely controlled by this biological recycling (Fig. 5). It is the litterfall that restitues large amounts of biologically precipitated Si to the soil system (high α_{BSi} in Eq. 11). This implies an increased availability (or large pool) of easily dissolvable Si. Decomposition of the thick humus layer will also provide organic acids and dissolved organic matter to the soil solution [97], which enhances the Si dissolution (Eq. 12). The effect will be most important for mineral dissolution, as forests soils are typically acidic (Eq. 12), but differ depending on tree-stand compositions, e.g. pH is lower in coniferous forests than in deciduous forests [89]. In contrast to favoured dissolution conditions, DSi uptake is quite important [72, 98, 99] and could potentially buffer increased mineral weathering [90, 100]. However vegetation uptake is not proven to be an active process in forests [101], r_A (Eq. 17) was thus neglected for forests in Fig. 5.

From a detailed study in temperate deciduous and coniferous forest soils [102], ASi contents (wt%) showed a decreasing trend with depth from the humus layer, topsoil (0–7.5 cm) and at depth (30–45 cm) with respectively 0.5–1.4 % ASi (at soil pH 3.8), 0.3–0.6 % ASi (at soil pH 3.8) and 0.3–0.4 % ASi (at soil pH 4.5). Dissolved organic carbon concentration, used as proxy for the organic acid concentration, in soil solution decreased with depth, 23.5–69 mg/l in the humus layer (at soil solution pH 4.12–5.05) and 2.3–3.7 mg/l at 60 cm depth (at soil solution pH 4.75–5.52). The DSi

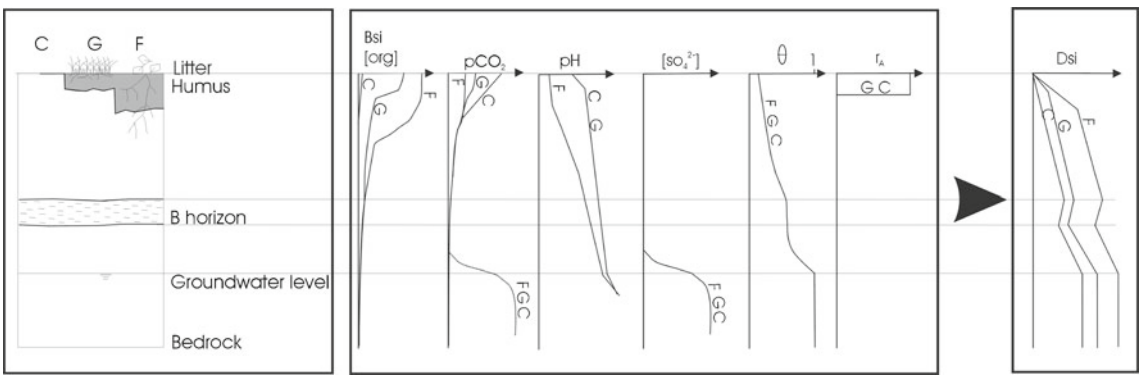

Fig. 5 Relative importance of the parameters (BSi, [org], pCO2, pH, $[SO_4^{2-}]$, $[CO_3^{2-}]$, θ, r_A) influencing the DSi concentrations in natural waters of forests (F), grasslands (G) and croplands (C); parameters influence Eqs. 10 and 12

concentration in the leachates of these horizons showed opposite trends and increased with depth, concentrations of 30.6–64.5 μM were measured in the humus layer and concentrations of 60.2–80.8 μM at 60 cm depth. These observations conform with Eq. 12, our representation in Fig. 5 and our conceptual model in Fig. 4 (even without the E-horizon).

4.1.2 Grasslands

Soil profiles of grasslands are characterized by shallow roots and a thin humus layer (Fig. 5). Grasses accumulate Si actively (Eq. 17), i.e. Si uptake is larger than water uptake [103]. In principle, the biological Si cycling in grasslands is more or less comparable with the biocycling of forests. The input of biogenic ASi in grassland soils is relatively high (high α_{ASi}. in Eq. 11) and comparable to forests. It varies from 55 to 67 kg Si ha^{-1} yr^{-1} for tall grass [104], which is comparable with inputs calculated for tropical forests (41–67 kg Si ha^{-1} yr^{-1} [98, 105] and from 22 to 26 kg Si ha^{-1} yr^{-1} for short grass [104], which is comparable with the inputs calculated for deciduous forests (22 kg Si ha^{-1} yr^{-1}) and higher than in coniferous forests (4.5 kg Si ha^{-1} yr^{-1}) [93]. But since grasses accumulate more Si (dry weight basis) and turnover at least as much Si as forests mineral weathering will be enhanced more severely in grasslands than in forests [104]. Different causes have been proposed for this relatively low bio recycling. Climatic weathering could be more important in forests enhancing dissolution processes [104] by influencing temperatures Eqs. 4 and 5 and soil moistures (Eq. 11). The lower specific surface (Eq. 12) of phytoliths could also explain the lower solubility (10–15 times) of grass ASi in comparison to forest ASi [106]. Due to intensive mowing, and possibly cattle grazing of grasslands in some regions, a part of the ASi pool is removed from the ecosystem [90]. In this case, the ASi accumulation in the soil will not be replenished (or restituted) by plant uptake, which could eventually result in depletion of easy dissolvable Si pool so that α_{ASi}. (Eq. 11) decreases. In contrast it has also been shown that grazing can lead to higher ASi in grasses [107, 108]. In field experiments, Blecker et al. [104] measured in different topsoils 0.2–0.5 g cm^{-2} soil organic C and 0.1–0.5 g cm^{-2} biogenic ASi. For the same soils at 70 cm depth, both parameters were $\leq$0.1 g cm^{-2}. This corresponds with our conceptual framework in which the biogenic ASi content diminishes like soil organic C with depth (Fig. 5, Eq. 12). Resulting DSi concentrations in natural waters are rather low compared with forest (last column in Fig. 5), which agrees with the observation of Struyf et al. [90].

4.1.3 Agriculture

In modern agriculture systems the biological recycling by vegetation, like occurring in forest and most grassland ecosystems, is severely disturbed. Croplands are subjected to tillage, harvesting, soil erosion and the use of fertilizers. All these management practices prevent either the accumulation of a humus layer (Fig. 5) or can lead to depletion of the mineral and amorphous Si pools in soils. The absence of biogenic ASi accumulation in cropland soils [109–111] leads to a low α_{ASi}.in Eq. 11. Seasonal crop and tillage practice reduces the contribution of root-induced weathering processes in rooting zone. The use of nitrate fertilizers enhances the weathering of Si as nitrification processes releases acids (Eq. 12) [57]. Moreover, often tillage techniques create the occurrence of a typical plough layer (between 0.15 and 0.3 m) with significant different physical, chemical and biological soil properties. Finally, erosion is important in croplands as bare soils are exposed to the wind and precipitation. Except, preventing a long-term accumulation of biogenic ASi in the top-soil layer, it also alters the DSi and ASi dynamics in cultivated first-order catchments [9]. While dissolved organic matter concentrations are the lowest in croplands compared to forests and grasslands, pCO_2 (Eq. 12) in soils was proved to be the highest [21] (Fig. 5). Resulting DSi concentrations in soil water are rather low (last column in Fig. 5) and it has been shown that base-flow delivery from agriculture catchments reflect these important changes in soil properties [90].

The general processes influencing the DSi concentrations for each type of land use are summarized in Fig. 5, and represent the state variables that determine the output of Eqs. 10 and 12. We assumed equal soil moisture profiles as soil water content is linked to the local hydrology (depth of the saturated zone) and less to the land use. This assumption allows focusing on the relative importance of the other state variables. Soil temperature (Eqs. 4 and 5) is generally lower under forest than under grassland cover [88]. Cropland soils have higher temperatures and seasonal variations are more important compared to the other land uses [88, 112]. As the measured temperature differences between cropland, grassland and forests are in the order of magnitude of a few degrees (°C), these differences will probably not influence directly the dissolution of Si but like stated previously can influence biological activity and thus the uptake of DSi (Eq. 17 if active), the amount of organic acids (Eq. 12), pCO_2 (Eq. 12), etc. However, as the root zone is deeper and humic layer thicker in forests, the amount of dissolved organic matter, used as a proxy for the organic acids

concentration, generally decreases from forests, grasslands to croplands [21]. Consequently, the pH (Eq. 12) is lower in forests than in grasslands and arable lands. Due to the lower pH, podzol soils develop more typically in forests [82] than in grasslands and croplands where no E-horizon is present. The pCO_2 (Eq. 12) in soils was proved to be the highest in arable land, followed by grasslands and lowest in forests [21]. In the saturated zone we assumed equal concentrations of sulphates and bicarbonates (pCO_2) for the three land uses as the soil profiles are developed in the same bedrock. To sum up, we can conclude that the acidity parameters (Eq. 12), which drive the dissolution are different according to land use, i.e. in forests organic acids and pH are important but in grassland and cropland pCO_2 will be more important.

4.2 Seasonal Climatic Variation

Seasonal variations of DSi have been observed in water of temperate forested catchments with humid winters and dry summers [92, 113]. Various explanations are given for the temporal variation in DSi transport [76, 92, 114] based on differences in 1) temperature; 2) biological uptake; 3) drainage regime and; 4) groundwater level. Seasonal temperature variation can affect biological activity and its related acid production and biological uptake. The decrease of DSi in natural waters during the growing season can be explained by the DSi uptake by vegetation [76] or by the consumption of DSi by diatoms in the river [92]. In the first case the decrease will be observed in soil waters in contrast to the second case where the decrease is only observed in river water. Gérard et al. [8] observed a significant seasonal variation in soil water and connectivity between the soil and river system, DSi concentrations in capillary soil solutions were generally ca. 35 μM lower during winter than during summer. When seasons change, evapotranspiration vary and precipitation patterns change, which leads to soil moisture variations. Consequently, this leads to different drainage regimes, at high soil moisture, conductivity will be high which lowers the residence time of the water. In that case, the contact time between Si-particles and water is short and less dissolution can take place. Changes of drainage regimes are often accompanied by groundwater fluctuations. If lithology of the aquifer varies vertically, more weatherable layers can be in contact with the higher groundwater levels of humid winters and release Si, in which case water chemistry can be correlated with groundwater level [114].

Applied on a typical growing season, and precipitation representative scale we would characterize two main periods, with typical processes influencing seasonal fluctuations. The first is the autumn-winter period with long low intensity precipitation, and low biological activity. A second is the spring-summer period with short heavy intensity rains, and coinciding with the growing seasons of forest, grassland and most crops. These seasons correspond with contrasting physical, chemical and biological settings that affect the Si buffer capacity in the soil-vegetation continuum.

In terms of climatology the spring-summer period has higher evapotranspiration rates which not only induce dryer soils, but also results in a higher DSi uptake by vegetation, illustrated as important soil-vegetation interaction in Fig. 6. Combined with less frequent but intensive rainfall events, high evapotranspiration leads to dryer conditions as represented by lower soil moisture states (θ in Fig. 6). It also causes reduced internal drainage and lower groundwater levels (Eqs. 9–11) limiting unsaturated DSi transport to the aquifer (Eq. 24). Like stated before, higher temperatures increases biological activity, which leads to more acid production (pH or H^+, [org] and pCO_2 in Fig. 6 and Eqs. 6–8 and 12). Consequently, higher acid production results in Si desorption and in a shift of cation exchange equilibria, i.e. base cations are replaced by H^+ on the mineral surfaces (Eqs. 6–8 and 12) [87]. This enhances Si weathering and ASi dissolution. At the end of the growing season when the vegetation diminishes uptake, DSi and other cation saturated conditions could occur and this could lead to the precipitation of hydroxialuminosilicates (HAS) [75, 80]. The formation of HAS is potentially an important sink for biologically recycled Si.

Other processes dominate the autumn-winter season. Low evapotranspiration rates induces low DSi uptake by passive vegetation, illustrated by a weak interaction between soil and vegetation for forest and grassland or no interaction in cropland in Fig. 6. Combined with the frequent long duration but low intensity rainfall and low evapotranspiration, it leads to higher soil moisture states (θ in Fig. 6), increased internal drainage and consequently to increased groundwater levels which can enhance dissolution of the lithologies (Eqs. 9–11). This period with low biological interaction coincides with the restitution of litter. The decaying organic matter releasing biogenic ASi into the soil giving a larger fresh ASi stock available, especially in forests where litterfall is important (ASi in Fig. 6). Cold temperatures could postpone the decay process till the start of spring, when temperatures rise and biological activity enhance decomposition. Further, cold periods

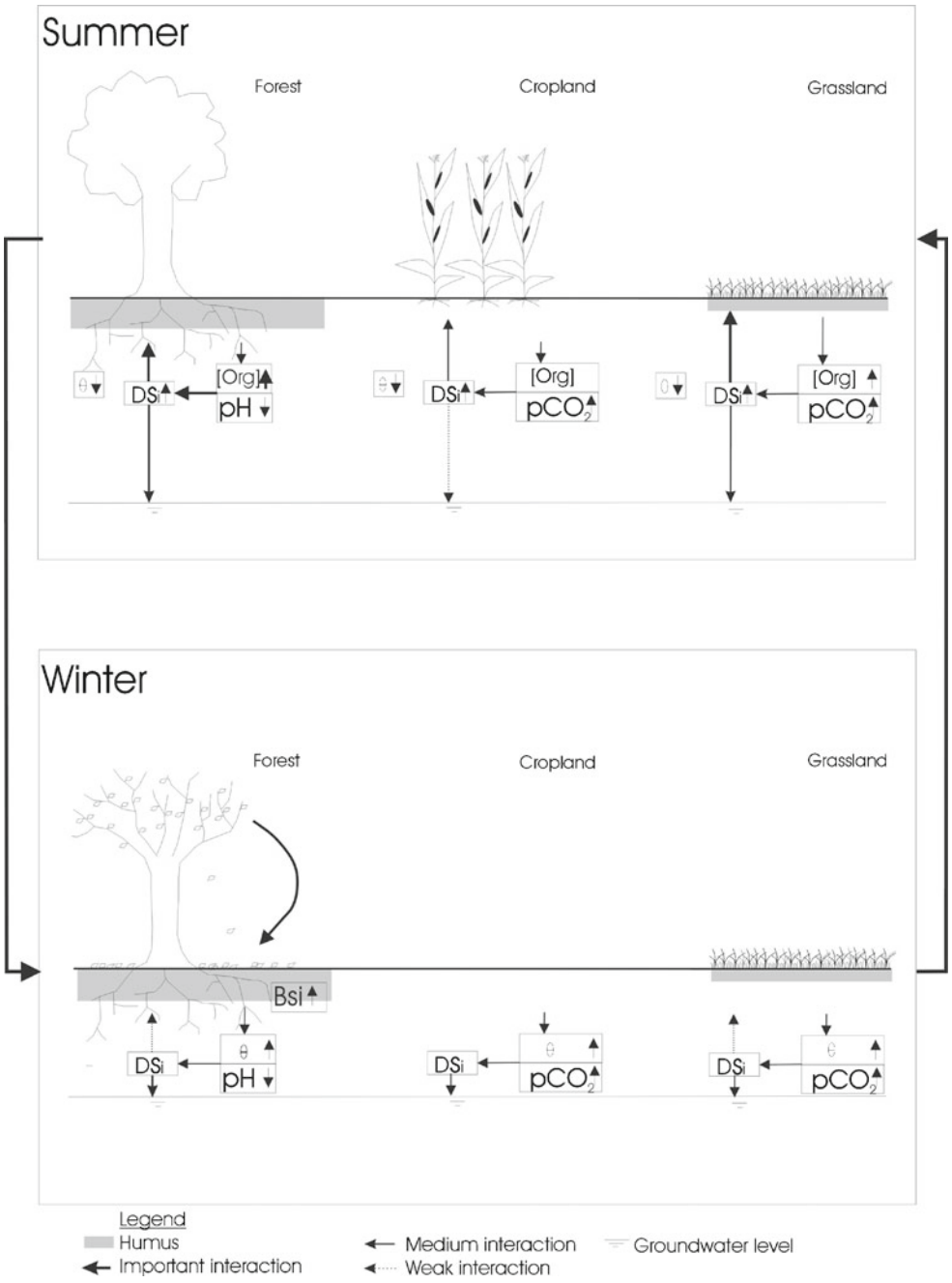

Fig. 6 Processes influencing the DSi dissolution in soils of forests, croplands and grasslands during summer and winter, assuming the same soil type for the three cases

could cause DSi polymerization and Si complexation with particulate material when water freezes [115]. Finally, hydroxialuminosilicates (HAS) formed during dry chemical saturated conditions dissolve in the wet soil moisture conditions and becomes a DSi source [75, 80].

To conclude, DSi concentrations should generally be lower during winter than during summer (e.g. observations in capillary solutions [8]), as acid production will drive a lot of processes enhancing Si dissolution. Transport processes in the dry summer will be slower, maximal DSi concentrations can be observed at different times in capillary soil water, leaching solution and river water due to diffusion processes from capillary to leaching solution [8] or due to a long transport time from soil to river. In the case that DSi concentrations reach saturation at the end of the summer, poorly cristalline Si phases

like HAS precipitates resulting in an increase of α_{HAS}. (Eq. 11).

5 Discussion and Conclusions

We presented a conceptual framework which describes DSi transport from land surface, through each soil horizon, subsurface until the river for catchments with temperate climate. This is the first time a framework of equations is proposed that may be used to develop a mechanistic model for DSi production and transport. To model DSi transport, a code should be written or existing codes (e.g. PHREEQC [116], MIN3P [78]) should be adapted to integrate all acidification factors (Eq. 12), sink processes (e.g. with Si adsorption with Eq. 14 and nanocolloid formation with Eqs. 15 and 16) and ASi pool (α_{ASi} in Eq. 11) which were often ignored in existing models. After coupling the chemical model to a water flux model, the proposed model needs to be validated by applying the model in field situation. As each field site has its own specific characteristics, the user of such the framework have to determine which controlling processes and rate limiting processes are important in his case study. Based on that analysis, the user can simplify the framework by dismissing some processes or simplify the soil profile representation (Fig. 4, e.g. elimination of horizons), if needed.

Several research gaps still impede full understanding of the Si cycle. On the scale of soil profiles, not all pedogenic processes are known. Influence of sulfates (SO_4^{2-}) in the saturated zone could potentially increase mobilisation [56, 57] and should be better studied to determine its relative importance. It is known that micro-organisms also play a role in the Si biogeochemical cycle. Landeweert et al. [117] observed that ectomycorrhizal fungi extract nutrients from minerals. Other studies showed micro-organisms can rework smectite clay mineral to the less Si-rich mineral illite [118] and attack biogenic ASi in plant roots [119]. Biogenic ASi reactivity has mostly been studied during laboratory experiments, while field information from soil profiles is lacking, it is required to specify the exact effect of chemical properties on ASi dissolution.

Through our conceptual model, we illustrated how sink and dissolution processes influencing Si transport can differ from one soil horizon to another for a typical podzol profile in a temperate climate. Our conceptual model (Fig. 4) is transformable to other soil types, as the elimination or incorporation of specific horizons is straightforward. This will allow simulating the effect of external forcings, i.e. seasonal variation and land use, on the internal dynamics of ecosystems. For example, by analysing the parameters driving DSi production (Eq. 12), one can study whether variation of DSi export is linked to biological activity.

ASi storage, Si-cycling and final Si-export differs for different land use types (forest, cropland, grassland). In a southern Swedish, undisturbed systems store a larger ASi amount, while cropland and grassland store lower ASi stocks. Easily soluble Si pools, representing the Si available upon contact with ionic active water, was lowest for croplands [10]. The latter corroborates the expected model output presented in Section 4.1 and Fig. 5 which accounts for the different ASi stocks but also for the different acids driving dissolution processes. Clymans et al. [10] concluded that historical land use changes probably has altered Si export from disturbed catchment, based on observed stock changes. This supported a study in the Scheldt basin where on the long-term base-flow Si export decreased from agriculture catchments [90]. The diminishing Si export can be explained by a perturbation of the vegetation-soil link, and changes in chemical properties of soils. The latter represents an alteration of the dissolution driving state variables (Eq. 12). For example, it is known that soil pH increases when forest becomes cropland or pasture and base-exchange properties increase [120]. To unravel the exact effect we propose to integrate our model in land use studies.

An important remaining question is how much DSi exported from a catchment finds it origin in ASi relative to mineral Si? To understand the relative contribution of the biological filter to eventual output of DSi, Derry et al. [121] successfully combined Ge/Si ratios with the Si concentrations. Cornelis et al. [4] recommended to make a Si mass balance and to combine the use of the geochemical tracers Ge/Si and δ^{30}Si as separation tools. Their applicability relies on distinct signatures characterizing the different sources within in the terrestrial Si cycle. For several dissolution processes, fractionation evidence is available [48]. Secondary clay mineral, plants and Fe-oxides preferentially include light Si isotopes, leading to similar signatures [122, 123], and making soil pore water enriched in heavy Si isotopes [123]. Secondary clay formation favours Ge uptake resulting in high Ge:Si ratios, while phytoliths are Ge selective (low Ge:Si ratio) [124–128] leading to a mixed Ge:Si signature in soil pore water depending on the relative contribution of these processes. The dissolution of ASi will alter the pore-water signature even further. Seasonal signature variation was observed in river water [4, 91] or soil water [80]. All these approaches are still in early stages of development,

therefore it is presently difficult to assess different Si sources based on either method. More detailed research on these tracers in specific land use types could significantly enhance this research. The results from such tracer studies will allow validating the controlling processes proposed by the future numerical models.

To assess CO_2 consuming processes like Si weathering [129] or diatom uptake, the exact quantification of silicate weathering (Fig. 2) in soils and total DSi delivery from the continent to the ocean are essential. In contrast to our proposed conceptual model, current approaches (e.g. [130]) ignore the biogenic Si pool as a DSi source or sink, as well as differences due to the land use types. Prediction models of global DSi transport in the future will have to take these factors into account as well as the expansion of agriculture [131]. It is expected that agricultural expansion has led, and will lead to a decrease in Si exchange between soils and rivers. Our model will be a useful tool to verify this hypothesis, to understand what controls this decrease and finally predict changes in Si export for different scenarios.

Acknowledgements Benedicta Ronchi and Wim Clymans would like to thank the Flemish Agency for the promotion of Innovation by Science and Technology (IWT) for funding PhD grants. Eric Struyf acknowledges FWO (Flemish Research Foundation) for funding his postdoc grant. We acknowledge FWO for funding project "Tracking the biological control on Si mobilization in upland ecosystems" (Project nr. G014609N) and BELSPO (Belgian Science Policy) for funding IAP SOGLO (P7/24). Floor Vandevenne and Ana Lúcia Pena Barão would like to thank BOF-UA for PhD fellowship funding.

References

1. Tréguer PJ, De La Rocha CL (2013) The world ocean silica cycle. Annu Rev Mar Sci 5:5.1–5.25
2. Ittekot V, Humborg C, Schäfer P (2000) Hydrological alterations and marine biogeochemistry: a silicate issue? Bioscience 50:776–782
3. Sommer M, Kaczorek D, Kuzyakov Y, Breuer J (2006) Silicon pools and fluxes in soils and landscapes-a review. J Plant Nutr Soil Sci 169:310–329
4. Cornelis J-T, Delvaux B, Georg RB, Lucas Y, Ranger J, Opfergelt S (2011) Tracing the origin of dissolved silicon transferred from various soil-plant systems towards rivers: a review. Biogeosciences 8:89–112
5. Sauer D, Saccone L, Conley DJ, Herrmann L, Sommer M (2006) Review of methodologies for extracting plant-available and amorphous Si from soils and aquatic sediments. Biogeochemistry 80:89–108
6. Laruelle GG, Roubeix V, Sferratore A, Brodherr B, Ciuffa D, Conley DJ, Dürr HH, Garnier J, Lancelot C, Le Thi Phuong Q, Meunier J-D, Meybeck M, Michalopoulos P, Moriceau B, Longphuirt SN, Loucaides S, Papush L, Presti M, Ragueneau O, Regnier P, Saccone L, Slomp CP, Spiteri C, Van Cappellen P (2009) Anthropogenic perturbations of the silicon cycle at the global scale: key role of the land-ocean transition. Glob Biogeochem Cycles 23:GB4031
7. Fraysse F, Pokrovsky OS, Schott J, Meunier JD (2006) Surface properties, solubility and dissolution kinetics of bamboo phytoliths. Geochim Cosmochim Acta 70:1939–1951
8. Gérard F, François M, Ranger J (2002) Processes controlling silica concentration in leaching and capillary soil solutions of an acidic brown forest soil (Rhône, France). Geoderma 107:197–226
9. Smis A, Van Damme S, Struyf E, Clymans W, Van Wesemael B, Frot E, Vandevenne F, Van Hoestenberghe T, Govers G, Meire P (2011) A trade-off between dissolved and amorphous silica transport during peak flow events (Scheldt river basin, Belgium): impacts of precipitation intensity on terrestrial Si dynamics in strongly cultivated catchments. Biogeochemistry 106:475–487
10. Clymans W, Struyf E, Govers G, Vandevenne F, Conley DJ (2011) Anthropogenic impact on amorphous silica pools in temperate soils. Biogeosciences. http://www.biogeosciences-discuss.net/8/4391/2011/bgd-8-4391-2011.pdf
11. Kurtz AC, Lugolobi F, Salvucci G (2011) Germanium-silicon as a flow path tracer: application to the Rio Icacos watershed. Water Resour Res 47:16
12. McDonnell JJ (1990) Rationale for old water discharge through macropores in a steep, humid catchment. Water Resour Res 26:2821–2832
13. Doucet F, Schneider C, Bones S, Kretchner A, Moss I, Tekely P, Exley C (2001) The formation of hydroxyaluminosilicates of geochemical and biological significance. Geochim Cosmochim Acta 65(15):2461–2467
14. Van Cappellen P (2003) Biomineralization and global biogeochemical cycles. In: Dove P, DeYoreo J, Weiner S (eds) Biomineralizations. Reviews in mineralogy and geochemistry 54:357–381. Mineral. Soc. Amer., Washington, DC. ISBN 093995066-9
15. McKeague JA, Cline MG (1963) Silica in soil solutions: II. The adsorption of monosilicic acid by soil and by other substances. Can J Soil Sci 43:83–96
16. Conrad CF, Icopini GA, Yasuhara H, Bandstra JZ, Brantley SL, Heaney PJ (2007) Modeling the kinetics of silica nanocolloid formation and precipitation in geologically relevant aqueous solutions. Geochim Cosmochim Acta 71:531–542
17. Jackson ML, Tyler SA, Willis AL, Bourbeau GA, Pennington RP (1948) Weathering sequence of clay-size minerals in soils and sediments. I. Fundamental generalizations. J Phys Colloid Chem 52:1237–1260
18. Bormann H, Klaassen K (2008) Seasonal and land use dependent variability of soil hydraulic and soil hydrological properties of two Northern German soils. Geoderma 145:295–302
19. Berner RA (1992) Weathering, plants and the long-term carbon cycle. Geochim Cosmochim Acta 56:3225–3231
20. Drever JI (1994) The effect of land plants on weathering rates of silicate minerals. Geochim Cosmochim Acta 58 (10):2325–2332
21. Albertsen M (1977) Labor- und Felduntersuchungen zum gasaustausch zwischen Grundwasser und Atmosphäre über natürlichen und verunreinigten Grundwässern. Thesis, Univ. Kiel
22. Street-Perrott FA, Barker PA (2008) Biogenic silica: a neglected component of the coupled global continental biogeochemical cycles of carbon and silicon. Earth Surf Process Landf 33:1436–1457
23. Scanlon TM, Raffensperger JP, Hornberger GM (2001) Modeling transport of dissolved silica in a forested headwater catchment: implications for defining the hydrochemical

response of observed flow pathways. Water Resour Res 37(4):1071–1082
24. Iler RK (1979) The chemistry of silica: solubility, polymerization, colloid and surface chemistry, and biochemistry. John Wiley & Sons, New York, 866 p
25. Drees LR, Wilding LP, Smeck NE, Senkayi AL (1989) In: Dixon B, Weed SB (eds) Minerals in soil environments, 2nd edn. Soil Sci Soc Am J, Madison, Wisconsin
26. Wada K (1989) In: Dixon JB, Weed SB (eds) Minerals in soil environments. SSSA Book series No.1, Madison
27. Matichenkov VV, Bocharnikova EA (2001) In: Datnoff LE, Snyder GH, Korndörfer GH (eds) Silicon in agriculture. Studies in Plant Science 8, Elsevier, Amsterdam
28. Chadwick OA, Hendricks DM, Nettleton WD (1987) Silica in duric soils, 2. Mineralogy, Soil Sci Soc Am J 51(4): 982–985
29. Struyf E, Conley DJ (2008) Silica: an essential nutrient in wetland biogeochemistry. Front Ecol Environ 6. doi:10.1890/070126
30. Aoki Y, Hoshino M, Matsubara T (2007) Silica and testate amoebae in a soil under pine-oak forest. Geoderma 142 (1–2):29–35
31. Stumm W, Wollast R (1990) Coordination chemistry of weathering: kinetics of the surface-controlled dissolutidn of oxide minerals. Rev Geophys 28:53–69
32. Dietzel M (2002) Dissolution of silicates and the stability of polysilicic acid. Geochim Cosmochim Acta 64(19): 3275–3281
33. Appelo CAJ, Postma D (1993) Geochemistry, groundwater, and pollution. A.A. Balkema, Rotterdam
34. Bowser CJ, Jones BF (2002) Mineralogical controls on the composition of natural waters dominated by silicate hydrolysis. Am J Sci 302:582–662
35. Dove PM (1995) Kinetic and thermodynamic controls on silica reactivity in weathering environments. In: Chemical weathering rates of silicate minerals. Mineralogical Society of America and the Geochemical Society. Rev Mineral Geochem 31:235–290
36. Dove PM, Crerar DA (1990) Kinetics of quartz dissolution in electrolyte solutions using a hydrothermal mixed flow reactor. Geochim Cosmochim Acta 54:955–969
37. Graf T, Therrien R (2007) Coupled thermohaline groundwater flow and single-species reactive solute transport in fractured porous media. Adv Water Resour 30:742–771
38. Dove PM (1999) The dissolution kinetics of quartz in aqueous mixed cation solutions. Geochim Cosmochim Acta 63(22):3715–3727
39. Sverdrup HU, Warfvinge P (1988) Weathering of primary silicate minerals in the natural soil environment in relation to a chemical weathering model. Water Air Poll 38:387–408
40. Sverdrup HU (1990) The kinetics of base cation release due to chemical weathering. Lund Univ. Press, Sweden, 246 p. ISBN 0-86238-247-5
41. Aagaard P, Helgeson HC (1982) Thermodynamic and kinetic constraints on reaction rates among mineral and aqueous solutions – I. Theoretical considerations. Am J Sci 282:237–285
42. Helgeson HC, Murphy WM, Aagaard P (1984) Thermodynamic and kinetic constraints on reaction rates among minerals and aqueous solution-II. Rate constants, effective surface area and the hydrolysis of feldspar. Geochim Cosmochim Acta 48:2405–2432
43. Chou L, Wollast R (1985) Steady-State kinetics and dissolution mechanisms of albite. Am J Sci 285:963–993
44. Holland H, Lazar B, Mc Gaffrey M (1986) Evolution of the atmosphere and the oceans. Nature 320:27–33
45. Berg A, Banwart SA (2000) Carbon dioxide mediated dissolution of Ca-feldspar: implications for silicate weathering. Chem Geol 163(1–4):25–42
46. Pokrovski GS, Schott J (1998) Experimental study of the complexation of silicon and germanium with aqueous organic species: Implications for germanium and silicon transport and Ge/Si ratio in natural waters. Geochim Cosmochim Acta 62(21/22):3413–3428
47. Oelkers EH, Schott J (1999) Experimental study of kyanite dissolution rates as a function of chemical affinity and solution composition. Geochim Cosmochim Acta 63(6):785–797
48. Opfergelt S, Cardinal D, André L, Delvigne C, Bremond L, Delvaux B (2010) Variations of δ^{30}Si and Ge/Si with weathering and biogenic input in tropical basaltic ash soils under monoculture. Geochim Cosmochim Acta 74: 225–240
49. Gautier JM, Oelkers EH, Schott J (1994) Experimental study of K-feldspar dissolution rates as a function of chemical affinity at 150 °C and pH 9. Geochim Cosmochim Acta 58:4549–4560
50. Devidal JL (1994) Solubilité et cinétique de dissolution/précipitation de la kaolinite en milieu hydrothermal. Approche expérimentale et modélisation. Ph. D. Thesis University Paul Sabatier, Toulouse, France
51. Devidal JL, Dandurand JL, Schott J (1992) In: Kharaka YK, Maest AS (eds) Water rock interaction. A. A. Balkema, Rotterdam
52. Devidal JL, Schott J, Dandurand JL (1997) An experimental study of kaolinite dissolution and precipitation kinetics as a function of chemical affinity and solution composition at 150 °C, 40 bars, and pH 2, 6.8, and 7.8. Geochim Cosmochim Acta 61:5165–5186
53. Murphy WM, Pabalan RT, Prikryl JD, Goulet CJ (1996) Reaction kinetics and thermodynamics of aqueous dissolution and growth of analcime and Na-clinoptilolite at 25 °C. Am J Sci 296:128–186
54. Andrews J, Schlesinger W (2001) Soil CO_2 dynamics, acidification, and chemical weathering in a temperate forest with experimental CO_2 enrichment. Glob Biogeochem Cycles 15:149–162
55. Taylor LL, Leake JR, Quirk J, Hardy K, Banwart SA, Beerling DJ (2009) Biological weathering and the long-term carbon cycle: integrating mycorrhizal evolution and function into the current paradigm. Geobiology 7:171–191
56. Lerman A, Wu LL, Mackenzie FT (2007) CO_2 and H_2SO_4 consumption in weathering and material transport to the ocean, and their role in the global carbon balance. Mar Chem 106:326–350
57. Klaminder J, Grip H, Mörth CM, Laudon H (2011) Carbon mineralization and pyrite oxidation in groundwater: importance for silicate weathering in boreal forest soils and stream base-flow chemistry. Appl Geochem 26:319–325
58. Farmer VC, Delbos E, Miller JD (2005) The role of phytolith formation and dissolution in controlling. Geoderma 127:71–79
59. Giesler R, Ilvesniemi H, Nyberg L, van Hees P, Starr M, Bishop K, Kareinen T, Lundstrfm US (2000) Distribution and mobilization of Al, Fe and Si in three podzolic soil profiles in relation to the humus layer. Geoderma 94: 249–263
60. Saccone L, Conley DJ, Sauer D (2006) Methodologies for amorphous silica analysis. J Geochem Explor 88:235–238
61. Van Cappellen P, Dixit S, van Beusekom J (2002) Biogenic silica dissolution in the oceans: Reconciling experimental and field-based dissolution rates. Glob Biogeochem Cycles 16. doi:10.1029/2001GB001431

62. Loucaides S, Behrends T, Van Cappellen P (2010) Reactivity of biogenic silica: Surface versus bulk charge density. Geochim Cosmochim Acta 74:517–530
63. Struyf E, Conley DJ (2012) Emerging understanding of the ecosystem silica filter. Biogeochemistry 107:9–18
64. Beckwith RS, Reeve E (1962) Studies on soluble silica in soils. I. The Sorption of silicic acid by soils and minerals. Aust J Soil Res 1(2):157–168
65. Hiemstra T, Barnett MO, van Riemsdijk WH (2007) Interaction of silicic acid with goethite. J Colloid Interface Sci 310:8–17
66. Hiemstra T, Van Riemsdijk WH (2002) On the relationship between surface structure and ion complexation of oxide-solution interfaces. In: Encyclopedia of surface and colloid science, 1st edn. Marcel Dekker Inc., New York. doi:WebQuery/wurpubs/122944
67. Rietra RP, Hiemstra T, Van Riemsdijk WH (2000) Electrolyte anion affinity and its effect on oxyanion adsorption on goethite. J Colloid Interface Sci 229:199–206
68. Rajasekaran R, Rajendiran KV, Kumar RM, Jayavel R, Dhanasekaran D, Ramasamy P (2003) Investigation of the nucleation kinetics of zinc thiourea chloride (ZTC) single crystals. Mater Chem Phys 82:273–280
69. Izumi S, Hara S, Kumagai T, Sakai S (2005). Molecular dynamics study of homogeneous crystal nucleation in amorphous silicon. J Cryst Growth 274:47–54
70. Madras G, McCoy BJ (2005) Nucleation, growth, and coarsening for two- and three-dimensional phase transitions. J Cryst Growth 279:466–476
71. Icopini GA, Brantley SL, Heaney PJ (2005) Kinetics of silica oligomerization and nanocolloid formation as a function of pH and ionic strength at 25 °C. Geochim Cosmochim Acta 69(2):293–303
72. Lucas Y (2001) The role of plants in controlling rates and products of weathering: importance of biological pumping. Annu Rev Earth Planet Sci 29:135–163
73. Exley C (1998) Silicon in life: a bioinorganic solution to bioorganic essentiality. J Inorg Biochem 69:139–144
74. Huang PM (1991) Ionic factors affecting the formation of short-range ordered aluminosilicates. Soil Sci Soc Am J 55:1172–1180
75. Turpault M-P, Righi D, Utérano C (2008) Clay minerals: precise markers of the spatial and temporal variability of the biogeochemical soil environment. Geoderma 147:108–115
76. Fulweiler RW, Nixon SW (2005) Terrestrial vegetation and the seasonal cycle of dissolved silica in a southern New England coastal river. Biogeochemistry 74:115–130
77. Gérard F, Mayer KU, Hodson MJ, Ranger J (2008) Modelling the biogeochemical cycle of silicon in soils: application to a temperate forest ecosystem. Geochim Cosmochim Acta 72:741–758
78. Mayer KU, Frind EO, Blowes DW (2002) Multicomponent reactive transport modeling in variably saturated porous media using a generalized formulation for kinetically controlled reactions. Water Resour Res 38:1174–1195
79. van Hees PAW, Lundström US, Giesler R (2000) Low molecular weight organic acids and their Al-complexes in soil solution-composition, distribution and seasonal variation in three podzolized soils. Geoderma 94:173–200
80. White AF, Vivit DV, Schulz MS, Bullen TD, Evett RR, Aagarwal J (2012) Biogenic and pedogenic controls on Si distributions and cycling in grasslands of the Santa Cruz soil chronosequence, California. Geochim Cosmochim Acta 94:72–94
81. Jury W, Horton R (2004) Soil physics, 6th edn. John Wiley & Sons, New York, 370 p
82. FAO, Food and Agriculture Organization (2001) Lecture notes ont the major soils of the world. World Soil Resour Rep http://www.fao.org/docrep/003/Y1899E/Y1899E00.HTM
83. Bormann BT, Wang D, Bormann FH, Benoit G, April R, Snyder MC (1998) Rapid, plant-induced weathering in an aggrading experimental ecosystem. Biogeochemistry 43:129–155
84. Moulton KL, West J, Berner RA (2000) Solute flux and mineral mass balance approaches to the quantification of plant effects on silicate weathering. Am J Sci 300:539–570
85. Bear J (1988) Dynamics of fluids in porous media. Elsevier, New York
86. Freeze RA, Cherry JA (1979) Groundwater. Prentice Hall, Englewood Cliffs, NJ
87. Berner RA, Rao JL, Chang S, O'Brien R, Keller CK (1998) Seasonal variability of adsorption and exchange equilibria in soil waters. Aquat Geochem 4:273–290
88. Savva Y, Szlavecz K, Pouyat RV, Groffman PM, Heisler G (2009) Effects of land use and vegetation cover on soil temperature in an urban ecosystem. Soil Sci Soc Am J 74: 469–480
89. Johanson E, Sandèn P, Öberg G (2003) Organic chlorine in deciduous and coniferous forest soils in Southern Sweden. Soil Sci 168(5):347–355
90. Struyf E, Smis A, van Damme S, Garnier J, Govers G, van Wesemael B, Conley DJ, Batelaan O, Frot E, Clymans W, Vandevenne F, Lancelot C, Goos P, Meire P (2010) Historical land use change has lowered terrestrial silica mobilization. Nat Commun 1(129). doi:10.1038/ncomms1128
91. Engström E, Rodushkin I, Ingri J, Baxter DC, Ecke F, Österlund H, Öhlander B (2010) Temporal isotopic variations of dissolved silicon in a pristine boreal river. Chem Geol 271:142–152
92. Neal C, Jarvie HP, Neal M, Love AJ, Hill L, Wickham H (2005) Water quality of treated sewage effluent in a rural area of the upper Thames Basin, southern England, and the impacts of such effluents on riverine phosphorus concentrations. J Hydrol 304:103–117
93. Bartoli F (1983) The biogeochemical cycle of silicon in two temperate forest ecosystems. Environ Biogeochem Ecol Bull 35:469–476
94. Cornelis J-T, Ranger J, Iserentant A, Delvaux B (2010) Tree species impact the terrestrial cycle of silicon through various uptakes. Biogeochemistry 97:231–245
95. Markewitz D, Richter D (1998) The bio in aluminium and silicon geochemistry. Biogeochemistry 42:235–252
96. Conley DJ (2002) Terrestrial ecosystems and the global biogeochemical silica cycle. Glob Biogeochem Cycles 16(4):1121. doi:10.1029/2002GB001894
97. Petersen L (1976) In: Hutchinson TC, Havas M (eds) Effects of acid precipitation on terrestrial ecosystems. Plenum, New York
98. Alexandre A, Meunier J-D, Colin F, Koud J-M (1997) Plant impact on the biogeochemical cycle of silicon and related weathering processes. Geochim Cosmochim Acta 61(3):677–682
99. Meunier J-D, Colin F, Alarcon C (1999) Biogenic silica storage in soils. Geology 27:835–838
100. Carey JC, Fulweiler R (2012) Watershed land use alters riverine silica cycling. Biogeochemistry. doi:10.1007/s10533-012-9784-2
101. Cornelis J-T, Delvaux B, Titeux H (2010) Contrasting silicon uptakes by coniferous trees: a hydroponic experiment on young seedlings. Plant Soil 336:99–106
102. Cornelis J-T, Delvaux B, Cardinal D, André L, Ranger J, Opfergelt S (2010) Tracing the mechanisms controlling

the release of dissolved silicon in forest soil solutions using Si isotopes and Ge/Si ratios. Geochim Cosmochim Acta 74:3913–3924
103. Marschner H (1995) Mineral nutrition of higher plants, 2nd edn. Academic Press, London
104. Blecker SW, McCulley RL, Chadwick OA, Kelly EF (2006) Biologic cycling of silica across a grassland bioclimosequence. Glob Biogeochem Cycles 20. doi:10.1029/2006GB002690
105. Lucas Y, Luizao FJ, Chauvel A, Rouiller J, Nahon D (1993) The relation between biological activity of the rain forest and mineral composition of soils. Science 260:521–523
106. Wilding LP, Drees LR (1974) Contributions of forest opal and associated crystalline phases of fine silt and clay fractions of soils. Clay Clay Miners 22:295–306
107. Massey FP, Hartley SE (2006) Experimental demonstration of the antiherbivore effects of silica in grasses: impacts on foliage digestibility and vole growth rates. Proc R Soc B 273:2299–2304
108. Melzer SE, Knapp AK, Kirkman KP, Smith MD, Blair JM, Kelly EF (2010) Fire and grazing impacts on silica production and storage in grass dominated ecosystems. Biogeochemistry 97:263–278
109. Opfergelt S, Delvaux B, André L, Cardinal D (2008) Plant silicon isotopic signature might reflect soil weathering degree. Biogeochemistry 91:163–175
110. Meunier, J-D, Guntzer F, Kirman S, Keller C (2008) Terrestrial plant-Si and environmental changes. Mineral Mag 72:263–267
111. Vandevenne F, Struyf E, Clymans W, Meire P (2012) Agricultural silica harvest: have humans created a new and important loop in the global silica cycle? Research Communications. Front Ecol Environ 10:243–248
112. Tejedor M, Jiménez C, Rodríguez M, Morillas G (2004) Effect of soil use change on soil temperature regime ISCO 2004 - 13th International Soil Conservation Organisation Conference – Brisbane, July 2004 Conserving Soil and Water for Society: Sharing Solutions
113. Likens GE, Bormann FH, Johnson NM, Fisher DW, Pierce RS (1970) Effects of forest cutting and herbicide treatment on nutrient budgets in the hubbard brook watershed-ecosystem. Ecol Monogr 40(1):23–47
114. Rice KC, Bricker OP (1995) Seasonal cycles of dissolved constituents in streamwater in two forested catchments in the mid-Atlantic region of the eastern USA. J Hydrol 170 (1–4):137–158
115. Tallberg P, Hartikainen H, Kairesalo T (1997) Why is soluble silicon in interstitial and lake water samples immobilized by freezing? Water Res 31(1):130–134
116. Parkhurst DL, Appelo CAJ (1999) User's guide to PhreeqC (Version 2)—a computer program for speciation, batch-reaction, one-dimensional transport, and inverse geochemical calculations, U.S. Geological Survey, Water-Resources Investigations Report 99–4259, Denver, CO
117. Landeweert R, Hoffland E, Finlay RD, Kuyper TW, van Breemen N (2001) Linking plants to rocks: ectomycorrhizal fungi mobilize nutrients from minerals. Trends Ecol Evol 16–25:248–254
118. Kim J, Dong H, Seabaugh J, Newell JS, Eberl DD (2004) Role of microbes in the smectite-to-illite reaction. Science 303:830–832
119. Watteau F, Villemin G (2001) Ultrastructural study of the biogeochemical cycle of silicon in the soil and litter of a temperate forest. Eur J Soil Sci 52:385–396
120. Reiners WA, Bouwman AF, Parsons WFJ, Keller M (1994) Tropical rain forest conversion to pasture: changes in vegetation and soil properties. Ecol Appl 4:363–377
121. Derry LA, Kurtz AC, Ziegler K, Chadwick OA (2005) Biological control of terrestrial silica cycling and export fluxes to watersheds. Nature 728:433
122. Douthitt CB (1982) The geochemistry of the stable isotopes of silicon. Geochim Cosmochim Acta 46:1449–1458
123. Opfergelt S, Cardinal D, Henriet C, Draye X, André L, Delvaux B (2006a) Silicon isotopic fractionation by banana (Musa spp.) grown in a continuous nutrient flow device. Plant Soil 285:333–345. doi:10.1007/s11104-006-9019-1
124. Murnane RJ, Stallard RF (1990) Germanium of silicon of the rivers of the Orinoco drainage basin. Nature 344: 749–752
125. Kurtz AC, Derry LA, Chadwick OA (2002) Germanium-silicon fractionation in the weathering environment. Geochim Cosmochim Acta 66:1525–1537
126. Scribner AM, Kurtz AC, Chadwick OA (2006) Germanium sequestration by soil: targeting the roles of secondary clays and Feoxyhydroxides. Earth Planet Sci Lett 243:760–770
127. Blecker SW, King SL, Derry LA, Chadwick OA, Ippolito JA, Kelly EF (2007) The ratio of germanium to silicon in plant phytoliths: quantification of biological discrimination under controlled experimental conditions. Biogeochemistry 86:189–199
128. Delvigne C, Opfergelt S, Cardinal D, Delvaux B, Andre L (2009) Distinct silicon and germanium pathways in the soil-plant system: evidence from banana and horsetail. J Geophys Res 114:G02013. doi:10.1029/2008JG000899
129. Chadwick OA, Kelly EF, Merritts DM, Amundson RG (1994) Atmospheric carbon dioxide consumption during soil development. Biogeochemistry 24:115–127
130. Goddéris Y, François LM, Probst A, Schott J, Moncoulon D, Labat D, Viville D (2006) Modelling weathering processes at the catchment scale: the WITCH numerical model. Geochim Cosmochim Acta 70:1128–1147
131. Gordon LJ, Peterson GD, Bennett EM (2008) Agricultural modifications of hydrological flows create ecological surprises. Trends in Ecol Evol 23:211–219